Gas-Phase Organometallic Kinetics: Substitution of CO for C_2H_4 in $Fe(CO)_3(C_2H_4)_2$

Bruce H. Weiller,[†] Michael E. Miller,[‡] and Edward R. Grant*[§]

Contribution from the Department of Chemistry, Baker Laboratory, Cornell University, Ithaca, New York 14853. *Received July 2, 1986*

Abstract: Gas-phase $Fe(CO)_3(C_2H_4)_2$ is observed to react thermally with CO at 297 K to form $Fe(CO)_4(C_2H_4)$ by the mechanism of dissociative substitution. From the CO and ethylene pressure dependencies of the observed reaction rate, the unimolecular decay constant for $Fe(CO)_3(C_2H_4)$ is found to be $2.9 \pm 0.3 \times 10^{-3}$ s^{-1}. In addition, the elementary branching ratio for the reaction of coordinatively unsaturated $Fe(CO)_3(C_2H_4)$ with CO or with ethylene is found to be 35 ± 5, favoring reaction with CO. The most stable form of $Fe(CO)_3(C_2H_4)$ is calculated by the extended Hückel method. The preference of $Fe(CO)_3(C_2H_4)$ for reaction with CO over C_2H_4 can be explained in part by statistical considerations.

Although bisolefin–iron tricarbonyl complexes fulfill the eighteen electron rule, they are unstable and cannot be isolated in the absence of excess olefin.[1,2] Recently complexes of this type have been implicated in the catalysis of olefin isomerization by iron pentacarbonyl. Grevels et al. showed that synthetic (*cis*-cyclooctene)$_2$Fe(CO)$_3$ will catalyze pentene isomerization at room temperature.[3] Others have observed IR bands in iron pentacarbonyl catalytic mixtures that now appear to be bisolefin complexes.[4]

We have been interested for some time in homogeneous catalysis by photogenerated organometallic complexes.[5-9] Our work has focussed on the kinetics of elementary processes, where possible for isolated reactants. We have identified catalytic cycles that proceed entirely in the gas phase.[6-9] Under such conditions, kinetic parameters reflect intrinsic properties of the reactants and their isolated transformation, unobscured by solvent effects.[10]

In the course of our work on gas-phase ethylene hydrogenation we have obtained kinetic and spectroscopic evidence for the importance of bisethylene iron tricarbonyl as a reservoir for active catalyst. For example, we find fast, catalytic ethane production in the dark at room temperature when H_2 is added to a photoprepared sample of $Fe(CO)_3(C_2H_4)_2$ and C_2H_4. The absolute rate of ethane production is directly proportional to the partial pressure of $Fe(CO)_3(C_2H_4)_2$. Spectroscopic observation confirms the presence of the bisethylene complex in catalytic mixtures of $Fe(CO)_5$, C_2H_4, and H_2.[11] This metastable complex can, therefore, be expected to play an important role in the overall kinetics of gas-phase catalytic hydrogenation.

In mixtures dilute in bisethylene iron tricarbonyl, the principal decay route is replacement of ethylene by CO to form the stable monoethylene complex:

$$Fe(CO)_3(C_2H_4)_2 + CO \rightarrow Fe(CO)_4(C_2H_4) + C_2H_4 \quad (1)$$

A likely mechanism for this overall reaction is that of dissociative substitution.

The present work isolates this reaction for kinetic study. We confirm the stepwise dissociative substitution mechanism and report the room temperature rate constant for unimolecular loss of ethylene from saturated $Fe(CO)_3(C_2H_4)_2$ and the bimolecular rate constant for addition of CO to unsaturated $Fe(CO)_3(C_2H_4)$ relative to that for ethylene. An observed preference for CO addition by unsaturated $Fe(CO)_3(C_2H_4)$ is rationalized in terms of a simple statistical model.

Results

Irradiation of a gaseous mixture of $Fe(CO)_4(C_2H_4)$ and ethylene with near UV light (351 or 337 nm) changes the infrared absorption spectrum as shown in Figure 1. As is clear from the spectra, irradiation converts $Fe(CO)_4(C_2H_4)$ to a new complex, which can readily be identified as $Fe(CO)_3(C_2H_4)_2$, and liberates free CO. The IR bands for $Fe(CO)_4(C_2H_4)$ and $Fe(CO)_3(C_2H_4)_2$ are listed in Table I.[12-18] Over the period of time directly following irradiation, $Fe(CO)_3(C_2H_4)_2$ decays with concomitant reformation of $Fe(CO)_4(C_2H_4)$ as shown in Figure 2. The decay of $Fe(CO)_3(C_2H_4)_2$ and formation of $Fe(CO)_4(C_2H_4)$ are first order in time as demonstrated by the linear time dependence of $\ln |A - A_\infty|$ shown in Figure 3. The slopes of plots as in Figure 3 give phenomenological rate constants (k_{obsd}). These rate constants show a distinct dependence on ethylene and CO pressures (Table II). The CO pressure dependence shows k_{obsd} to increase to an asymptotic limit (Figure 4). In addition, k_{obsd} shows an inverse dependence on ethylene pressure (Figure 5).

Discussion

We follow the chemical evolution of a gas-phase mixture of CO, C_2H_4, and the photolabile complex $Fe(CO)_4(C_2H_4)$ as the system is irradiated and then allowed to relax thermally at 297 K. Irradiation cleanly converts $Fe(CO)_4(C_2H_4)$ and C_2H_4 to $Fe(CO)_3(C_2H_4)_2$ and CO. The bands for $Fe(CO)_4(C_2H_4)$ decrease in intensity while new bands form for $Fe(CO)_3(C_2H_4)_2$ (2069,

[†] Present address: Argonne National Laboratory, Chemistry Division, Argonne, IL 60439.
[‡] Present address: U.S. Dept. of Energy, Pittsburgh Energy Technology Center, Pittsburgh, PA 15236.
[§] Address correspondence to this author at Department of Chemistry, Purdue University, W. Lafayette, IN 47907.

(1) Elian, M.; Hoffman, R. *Inorg. Chem.* **1975**, *14*, 1058.
(2) Fleckner, H.; Grevels, F.-W.; Hess, D. *J. Am. Chem. Soc.* **1984**, *106*, 2027.
(3) Recent work has shown that $Fe(CO)_3(C_2H_4)_2$ is a very active catalyst for olefin isomerization at room temperature. Wuu, Y.-M.; Bentsen, J. G.; Brinkley, C. G.; Wrighton, M. S., manuscript submitted for publication.
(4) Chase, D. B.; Weigert, F. J. *J. Am. Chem. Soc.* **1981**, *103*, 977.
(5) Whetten, R. L.; Fu, K.-J.; Grant, E. R. *J. Am. Chem. Soc.* **1982**, *104*, 4270.
(6) Whetten, R. L.; Fu, K.-J.; Grant, E. R. *J. Chem. Phys.* **1983**, *79*, 2626.
(7) Miller, M. E.; Grant, E. R. *Applications of Lasers to Industrial Chemistry*; Kaldor, A., Woodin, R., Eds.; 1984; Vol. *458*, p 154.
(8) Miller, M. E.; Grant, E. R. *J. Am. Chem. Soc.* **1984**, *106*, 4635.
(9) Miller, M. E.; Grant, E. R. *J. Am. Chem. Soc.* **1985**, *107*, 3386.
(10) Picosecond studies have shown $Cr(CO)_5$ to interact with solvent within a 25 ps laser pulse. Welch, J. A.; Peters, K. S.; Vaida, V. *J. Phys. Chem.* **1982**, *86*, 1941.
(11) Miller, M. E.; Grant, E. R., manuscript in preparation.
(12) $Fe(CO)_4(C_2H_4)$ has been assigned C_{2v} symmetry (ref 13) which is consistent with the four carbonyl IR bands generally observed (ref 14-17). The only previously reported gas-phase carbonyl spectrum (ref 14) shows a band at 1988 cm^{-1} which we do not observe. We find a doublet at 2007 and 2002 cm^{-1} that we assign to be the gas-phase position of the fourth band. Our values for the low frequency metal–carbon stretch bands agree well with more recent values (Table I, ref 18).
(13) Davis, M. I.; Speed, C. S. *J. Organomet. Chem.* **1970**, *21*, 401.
(14) Andrews, D. C.; Davidson, G. *J. Organomet. Chem.* **1972**, *35*, 161.
(15) Murdoch, H. D.; Weiss, E. *Helv. Chim. Acta* **1963**, 1588.
(16) Bigorne, M. *J. Organomet. Chem.* **1978**, *160*, 345.
(17) Ellerhorst, G.; Gerhartz, W.; Grevels, F.-W. *Inorg. Chem.* **1980**, *19*, 67.
(18) Beach, D. B.; Jolly, W. L. *Inorg. Chem.* **1983**, *22*, 2137.

0002-7863/87/1509-0352$01.50/0

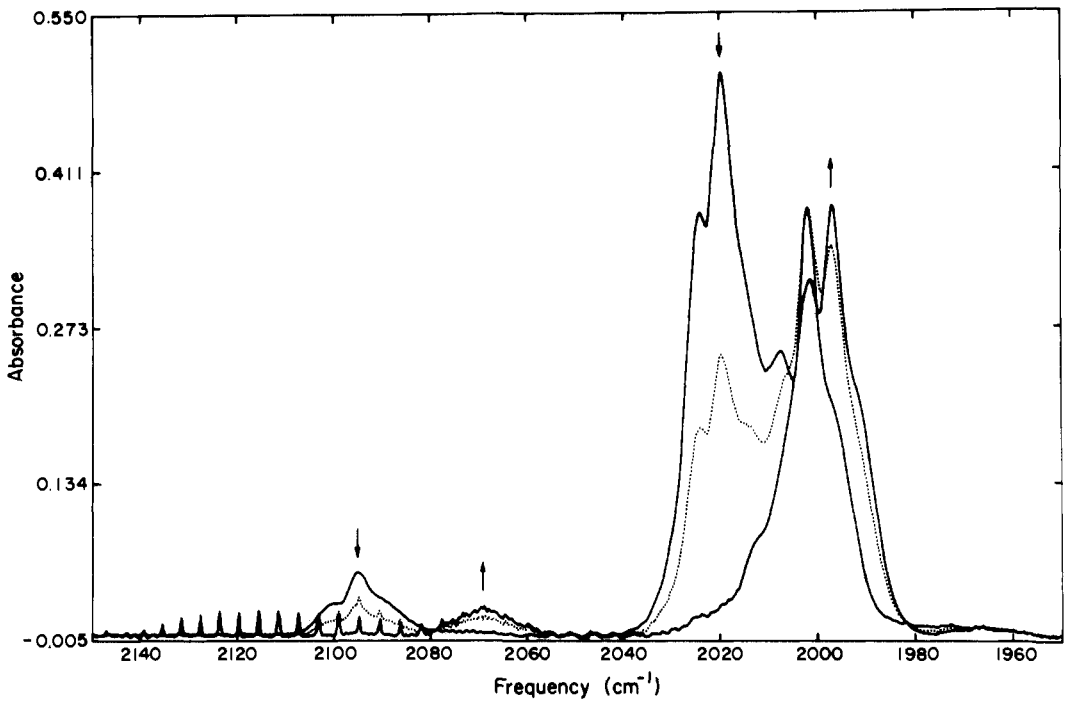

Figure 1. FTIR spectrum as a mixture of $Fe(CO)_4(C_2H_4)$ (0.300 torr) and ethylene (400 torr) is photolyzed. The arrows indicate growth or decay.

Table I. IR Absorptions of Olefin Iron Carbonyls

complex	conditions[a] (K)	frequencies (cm^{-1})[b]	ref
$Fe(CO)_4(C_2H_4)$	gas (298)	2095 (0.11), 2024 (0.74), 2020 (1.00) 2007 (0.50), 2002 (0.75) 706 (0.04), 636 (1.00), 592 (0.27) 494 (0.16), 458 (0.01)	this work
	gas (298)	2095 s, 2020 vs, 2003 vs, 1988 vs 708 m, 638 vs, 621 vs, 590 s, 540 w, 480 m, 430 m	14
	gas (298)	702, 633, 586, 488, 451	18
	CS_2 (298)	2081 s, 2002 vs, 1996 vs, 1970 vs	14
	fil (298))	2088 vs, 2013 sh, 2007 vs, 1986 vs	15
	hex (298)	2087 s, 2012 s, 2006 vs, 1985 s	16
	MCH (298)	2087 (0.13), 2013 sh, 2007 (1.00), 1984 (0.67)	3
	MCH (77)	2088 (0.18), 2011 sh, 2006 (1.00), 1980 (0.83)	3
	Ar (10)	2094, 2020, 2009, 1991	17
$Fe(CO)_3(C_2H_4)_2$	gas (298))	2069 (0.074), 2001 (0.80), 1997 (1.00)	this work
	MCH (273)	2060 (0.075), 1988 sh, 1981 (1.00)	3
	MCH (90)	2060 (0.83), 1988 (0.40), 1981 (1.00)	3
$Fe(CO)_3$(*cis*-cyclooctene)$_2$	hex (248)	2044 m, 1966 vs	2
$Fe(CO)_3$(*trans*-cyclooctene)$_2$	hex (298)	2046 m, 1982 s, 1971 vs	2
$Fe(CO)_3$(methyl acrylate)$_2$	hex (243)	2087 vw, 2024 vs, 2012 s	19

[a] gas = gas phase, hex = *n*-hexane, MCH = methylcyclohexane, CS_2 = carbon disulfide, fil = film, Ar = argon. [b] Relative in intensities in parentheses.

Table II. Observed Rate Constants

entry	CO (torr)	C_2H_4 (torr)	k_{obsd} (min^{-1}) formation	decay
1	1.55	100	0.0669 ± 0.0039	0.0733 ± 0.0046
2	1.56	202	0.0309 ± 0.00111	0.0291 ± 0.0012
3	1.55	400		0.0195 ± 0.0006
4	1.55	404	0.0226 ± 0.0006	0.0234 ± 0.0007
5	1.55	600	0.0144 ± 0.0005	0.0154 ± 0.0005
6	1.55	702	0.0110 ± 0.0004	0.00983 ± 0.00035
7	1.55	777	0.0105 ± 0.0007	0.0113 ± 0.0007
8	3.0	600	0.0237 ± 0.0008	0.0244 ± 0.0010
9	5.0	600	0.0365 ± 0.0014	0.0352 ± 0.0017
10	7.1	600	0.0489 ± 0.0018	0.0480 ± 0.0026
11	9.0	600	0.0602 ± 0.0022	0.0592 ± 0.0032

Table III. Derived Rate Constants

	k_1 (s^{-1})	k_3/k_2
k_{obsd} vs. [CO]	2.5 ± 0.2 × 10^{-1}	39.7 ± 3.5
k_{obsd} vs. [C_2H_4]	3.2 ± 0.2 × 10^{-1}	30.8 ± 3.0
mean	2.9 ± 0.3 × 10^{-1}	35 ± 5

2001, and 1997 cm^{-1}) and free CO. Accounting for matrix shifts, these agree well in position with those of matrix isolated $Fe(CO)_3(C_2H_4)_2$ as recently observed by Wuu et al.[3] In addition, the relative intensities match with the IR spectra for other known bisolefin–iron tricarbonyl complexes, all of which appear to have trigonal–bipyramidal structures with the olefins meridional (local C_{2v} symmetry).[2,19,20]

The relaxation of the system following irradiation exhibits well-behaved kinetics. The overall reaction is first-order in time, and the decay rate of $Fe(CO)_3(C_2H_4)_2$ matches the rate of formation of $Fe(CO)_4(C_2H_4)$ (Figure 3). Spectral amplitudes indicate that recovery of parent is complete. From these observations we conclude that competing reactions, such as CO insertion to form cyclopentanone, are not important in this system.[21-23]

(19) Grevels, F.-W.; Schulz, D.; Koerner von Gustorf, E. *Agnew. Chem., Int. Ed. Engl.* **1974**, *13*, 534.
(20) Grevels, F.-W.; Schneider, K.; Kruger, C.; Goodard, R. *Z. Naturforsch.* **1980**, B*35*, 360.
(21) Weissberger, E.; Laszlo, P. *Acc. Chem. Res.* **1976**, *9*, 209.
(22) Mantzaris, J.; Weissberger, E. *J. Am. Chem. Soc.* **1974**, *96*, 1880.
(23) Stockis, A.; Hoffmann, R. *J. Am. Chem. Soc.* **1980**, *102*, 2952 and references therein.

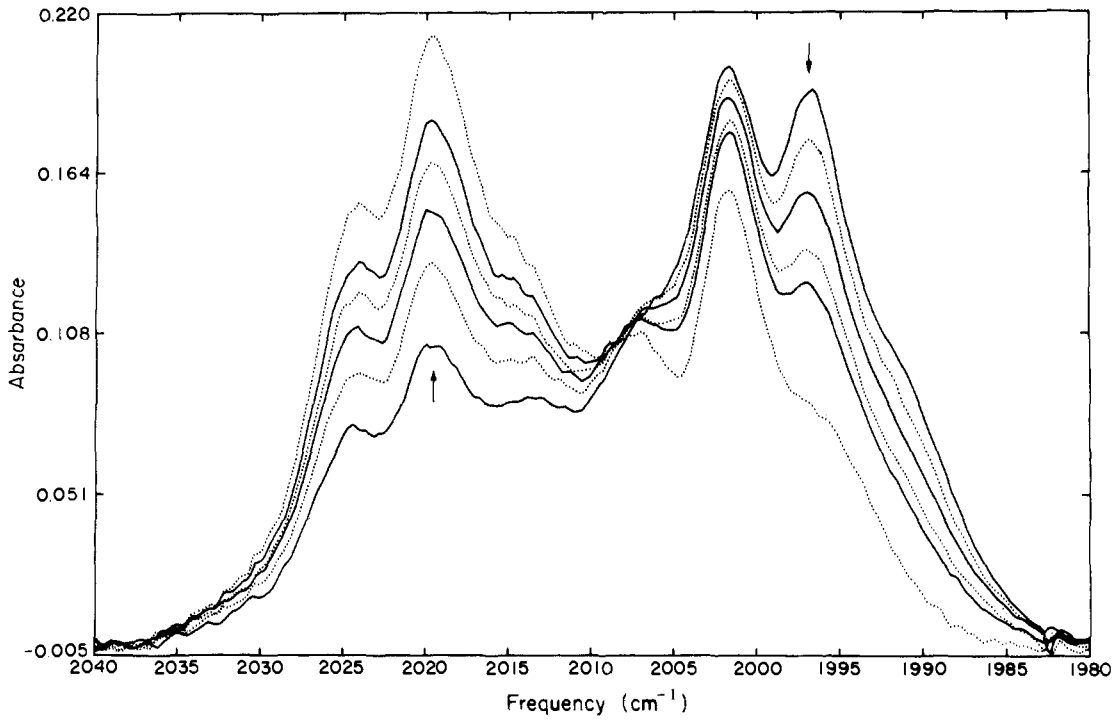

Figure 2. IR spectral changes as $Fe(CO)_3(C_2H_4)_2$ reacts with CO to form $Fe(CO)_4(C_2H_4)$. The time between the first and last spectrum is 19 min. Pressures of reagents are 0.050 ($Fe(CO)_4(C_2H_4)$), 200 (ethylene), and 1.50 torr (CO).

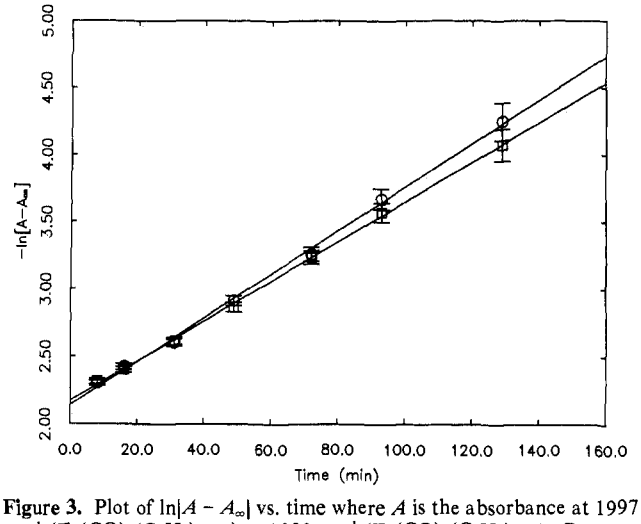

Figure 3. Plot of $\ln|A - A_\infty|$ vs. time where A is the absorbance at 1997 cm^{-1} ($Fe(CO)_3(C_2H_4)_2$, ○) or 2020 cm^{-1} ($Fe(CO)_4(C_2H_4)$, □). Reagent pressures are ($Fe(CO)_4(C_2H_4)$) 0.050, (CO) 1.50, and (ethylene) 600 torr. The lines are best weighted linear least-squares fits to the data. The slopes give k_{obsd}.

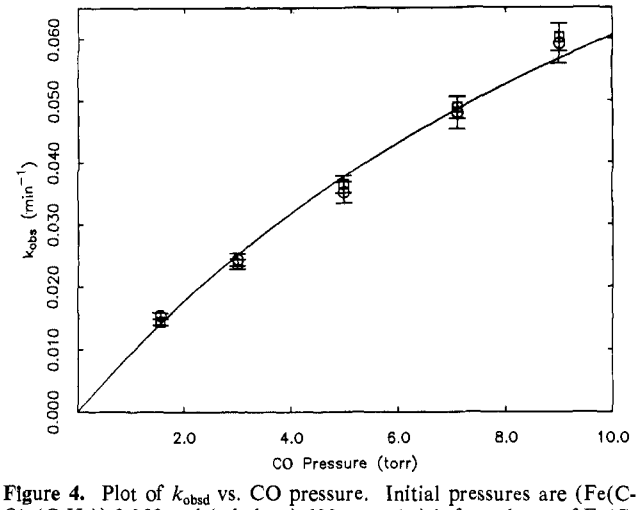

Figure 4. Plot of k_{obsd} vs. CO pressure. Initial pressures are ($Fe(CO)_4(C_2H_4)$) 0.050 and (ethylene) 600 torr. (○) is from decay of $Fe(CO)_3(C_2H_4)_2$ and (□) is from formation of $Fe(CO)_4(C_2H_4)$. The line is the best weighted nonlinear least-squares fit to the data assuming the functional form in eq 6.

Experiments have established that substitution processes in iron carbonyl complexes generally proceed via an initial step of dissociation.[24-31] Thus, the likely mechanism underlying reaction 1 is dissociative substitution.

$$Fe(CO)_3(C_2H_4)_2 \underset{k_2}{\overset{k_1}{\rightleftharpoons}} Fe(CO)_3(C_2H_4) + C_2H_4 \quad (2)$$

$$Fe(CO)_3(C_2H_4) + CO \xrightarrow{k_3} Fe(CO)_4(C_2H_4) \quad (3)$$

Adopting this mechanism and applying the steady-state assumption to $Fe(CO)_3(C_2H_4)$ yields a simple expression for the rate of decay of $Fe(CO)_3(C_2H_4)_2$

$$-\frac{d\{[Fe(CO)_3(C_2H_4)_2]\}}{dt} = \frac{k_1k_3[CO][Fe(CO)_3(C_2H_4)_2]}{k_2[C_2H_4] + k_3[CO]} = k_{obsd}[Fe(CO)_3(C_2H_4)_2] \quad (4)$$

In this work CO and ethylene are present in large excess and thus can be considered to have time independent concentrations, allowing eq 4 to be integrated directly to yield

$$[Fe(CO)_3(C_2H_4)_2] = [Fe(CO)_3(C_2H_4)_2]_0 \exp(-k_{obsd}t) \quad (5)$$

Mass balance gives the time dependence of $Fe(CO)_4(C_2H_4)$

$$[Fe(CO)_4(C_2H_4)] = [Fe(CO)_4(C_2H_4)]_0 + [Fe(CO)_3(C_2H_4)_2]_0\{1 - \exp(-k_{obsd}t)\} \quad (6)$$

(24) Angelici, R. J. *Organomet. Chem. Rev.* **1968**, *3*, 173.
(25) Howell, J. A. S.; Burkinshaw, P. M. *Chem. Rev.* **1983**, *83*, 557.
(26) Cardaci, G.; Narciso, V. *J. Chem. Soc., Dalton Trans.* **1972**, 2289.
(27) Burkinshaw, P. M.; Dixon, D. T.; Howell, J. A. S. *J. Chem. Soc., Dalton Trans.* **1980**, 999.
(28) Cardaci, G. *Inorg. Chem.* **1974**, *13*, 2974.
(29) Cardaci, G. *Inorg. Chem.* **1974**, *13*, 368.
(30) Cardaci, G. *Int. J. Chem. Kinet.* **1973**, *5*, 805.
(31) Cardaci, G. *J. Organomet. Chem.* **1974**, *76*, 385.

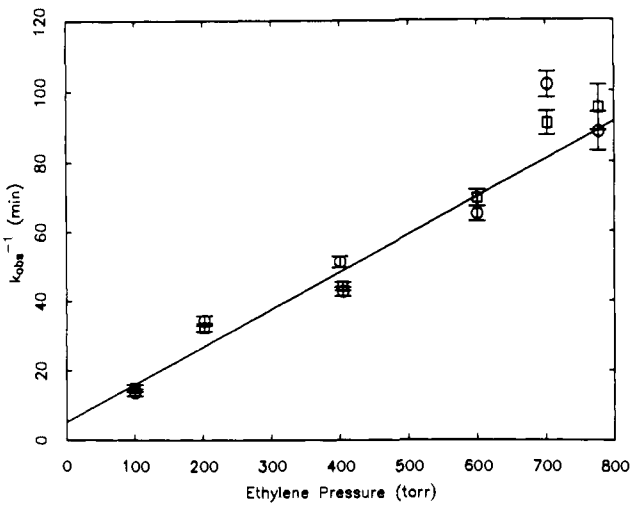

Figure 5. Plot of $(k_{obsd})^{-1}$ vs. ethylene pressure. Initial pressures are $(Fe(CO)_3(C_2H_4))$ 0.050 and (CO) 1.50 torr. (○) is from decay of $Fe(CO)_3(C_2H_4)_2$ and (□) is from formation of $Fe(CO)_4(C_2H_4)$. The line is the best weighted least-squares fit to the data.

Equations 5 and 6 predict a first-order time dependence for $[Fe(CO)_3(C_2H_4)_2]$ and $[Fe(CO)_4(C_2H_4)]$ as is found (Figure 3).

The above analysis also predicts an explicit dependence of k_{obsd} on CO and ethylene pressures:

$$k_{obsd} = \frac{k_1 k_2[CO]}{k_2[C_2H_4] + k_3[CO]} \quad (7)$$

Equation 7 says that k_{obsd} will increase to an asymptotic limit with increasing [CO]. Figure 4 shows the observed dependence of k_{obsd} on CO pressure. The solid line is the best nonlinear least-squares fit[32] to the functional form in eq 7, in good agreement with the proposed mechanism.

Equation 7 can be rearranged to yield a linear dependence for $(k_{obsd})^{-1}$ on ethylene pressure. Figure 5 shows that this is precisely the behavior observed.

$$\frac{1}{k_{obsd}} = \frac{k_2[C_2H_4]}{k_1 k_3[CO]} + \frac{1}{k_1} \quad (8)$$

From eq 7 and 8, the values of k_1, the unimolecular decay rate of $Fe(CO)_3(C_2H_4)_2$, and k_3/k_2, the branching ratio for reaction of $Fe(CO)_3(C_2H_4)$ with CO or ethylene, are obtained independently. Pairs of values presented in Table III fall within their respective experimental error. The average values are $k_1 = 2.9 \pm 0.3 \times 10^{-3}$ s^{-1} and $k_3/k_2 = 35 \pm 5$.

It is interesting to note that, on the basis of our mechanism and observed rate behavior, coordinatively unsaturated $Fe(CO)_3(C_2H_4)$ appears to intrinsically favor reaction with CO over ethylene by 35:1. Since this is a gas-phase result, it represents the true branching ratio, unbiased by any solvent cage effects.

The origin of this preference for CO can in part be rationalized on statistical grounds. Consider the structures of $Fe(CO)_4(C_2H_4)$, $Fe(CO)_3(C_2H_4)_2$, and $Fe(CO)_3(C_2H_4)$ (Figure 6a–c). $Fe(CO)_4(C_2H_4)$ has been determined by electron diffraction to be trigonal bipyramidal with the ethylene lying in the equatorial plane.[13] The expected geometry for $Fe(CO)_3(C_2H_4)_2$, based on the structures of analogous complexes[2,19,20] and theoretical expectations,[23] is trigonal bipyramidal with both ethylenes in the equatorial plane. We have calculated the lowest energy structure of $Fe(CO)_3(C_2H_4)$ by the extended Huckel method.[33] We find the most favorable geometry for coordinatively unsaturated $Fe(CO)_3(C_2H_4)$ to be square planar with the ethylene moiety perpendicular to the plane (Figure 6). This result agrees with the calculations of others[34] and is analogous to the structure of Zeise's salt $[Pt(Cl)_3(C_2H_4)^{1-}]$.[35]

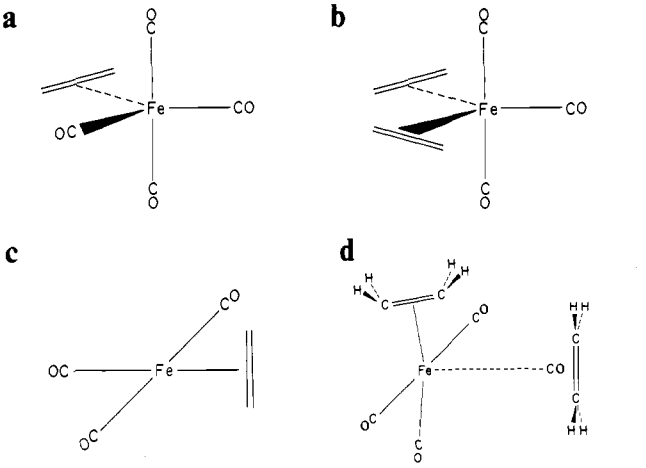

Figure 6. The structures of $Fe(CO)_4(C_2H_4)$ (a), $Fe(CO)_3(C_2H_4)_2$ (b), and $Fe(CO)_3(C_2H_4)$ (c). The attack of CO or C_2H_4 on $Fe(CO)_3(C_2H_4)$ is shown in (d). See text for description.

Now consider the approach of CO or ethylene to $Fe(CO)_3(C_2H_4)$. The attacking ligand must approach from above or below the square plane. The incoming ligand, the bound ethylene, and the CO trans to it will define the equatorial plane in the product $Fe(CO)_4(C_2H_4)$ or $Fe(CO)_3(C_2H_4)_2$ (Figure 6d). For either CO or ethylene recombination to occur, only bending-back of the ethylene and CO is required.[36] The high-energy process of ethylene rotation is avoided.[37] Thus we expect barriers to both recombinations to be small and, therefore, look to the preexponential factor to explain the branching ratio.

More specifically, it is instructive to hypothesize that the activation energies are the same, and the relative rate constant is expressed as a ratio of two transition-state theory rate preexponential factors.[38] Under such conditions the measured value for

$$k_3/k_2 = \exp(\Delta S_3^{\ddagger} - \Delta S_2^{\ddagger})/R = \exp\{\Delta(\Delta S^{\ddagger})\}/R \quad (9)$$

k_3/k_2 gives an experimental $\Delta(\Delta S^{\ddagger}) = 7.1 \pm 0.5$ eu. Any theoretical estimate of the activation entropy for recombination must account for the rotational degrees of freedom lost when free ligands are bound to the metal center. Such considerations predict a difference between the rates for CO and C_2H_4 addition simply on statistical grounds; C_2H_4 has one more rotational degree of freedom to lose. From rotational partition functions, the 297-K rotational entropy of free CO is 11.3 eu while that for ethylene is 15.9 eu.[39] The difference of 4.6 eu is a substantial fraction of our assumed experimental value of $\Delta(\Delta S^{\ddagger}) = 7.1$ eu. A full temperature study is underway to determine if there is an activation energy contribution to the branching ratio and to additionally obtain the dissociation energy for the unimolecular decay

$$Fe(CO)_3(C_2H_4)_2 \rightarrow Fe(CO)_3(C_2H_4) + C_2H_4$$

Experimental Section

$Fe(CO)_4(C_2H_4)$ is synthesized by the method of Murdoch and Weiss.[15] Briefly, a slurry of $Fe_2(CO)_9$ (Aldrich) in dry pentane is stirred

(32) Bevington, P. R. *Data Reduction and Error Analysis for the Physical Sciences*; McGraw-Hill: New York, 1969.

(33) Extended Huckel calculations performed with the ICON program obtained from R. Hoffmann. Bond lengths were taken from ref 13. All bond angles were varied systematically to obtain the lowest energy structures.

(34) Albright, T. A.; Clemens, P. R.; Hughes, R. P.; Hinton, D. E.; Margerum, L. D. *J. Am. Chem. Soc.* **1982**, *104*, 5369.

(35) Purcell, K. F.; Katz, J. C. *Inorganic Chemistry*; W. B. Saunders: Philadelphia, 1977; p 871.

(36) Recent matrix isolation experiments support this proposition (ref 3).

(37) Albright, T. A.; Hoffmann, R.; Thibeault, J. C.; Thorn, D. L. *J. Am. Chem. Soc.* **1979**, 101, 3801.

(38) Moore, J. W.; Pearson, R. G. *Kinetics and Mechanism*; John Wiley and Sons: New York, 1981; p 178.

(39) McQuarrie, D. A. *Statistical Mechanics*; Harper and Row: New York, 1976. Additional data for this calculation are taken from ref 40. The difference is, as expected, less then the difference in third-law entropy values at 298 K of 5.1 eu. F. D. Rossini, et al. *Selected Values of Chemical Thermodynamic Properties*; NBS Circular 500: Washington DC 1952.

(40) Herzberg, G. *Molecular Spectra and Molecular Structure II. Infrared and Raman Spectra of Polyatomic Molecules*; Van Nostrand Reinhold: 1945.

under 50 atm of ethylene for 48 h at room temperature. The resulting mixture is then distilled at reduced pressure to separate $Fe(CO)_5$ from $Fe(CO)_4(C_2H_4)$. The fraction of interest is collected at 34 °C and 12 torr. The IR spectrum confirms the absence of $Fe(CO)_5$. $Fe(CO)_4(C_2H_4)$ is stored at −78 °C in the dark.

For the kinetic experiments, samples are prepared on a standard, all glass high-vacuum line. Gas mixtures are prepared by the pile-on method. Typically the reagent pressures are 0.050 torr of $Fe(CO)_4(C_2H_4)$, 1.5–9.0 torr of CO (research grade, Matheson), and 100–800 torr of ethylene (CP grade, Matheson). Ethylene is purified by 3 freeze–pump–thaw cycles to remove volatile impurities. The photolysis source is a Lambda-Physik EMG-101 Excimer Laser used on either the XeF (351 nm) or N_2 (337 nm) lines. All kinetic runs use 337 nm. The FTIR spectrometer is an IBM Model IR 98. Typically the spectra are taken at 0.5-cm^{-1} resolution, averaging 10 scans. The ethylene and CO spectra are subtracted out. The temperature in all experiments is ambient (297 K).

Acknowledgment. We thank C.G. Brinkley and M.S. Wrighton for communicating their results prior to publication. Acknowledgment is made to the Donors of the Petroleum Research Fund, administered by the American Chemistry Society, for support of this research.

Registry No. $Fe(CO)_3(C_2H_4)_2$, 74278-01-6; $Fe(CO)_3(C_2H_4)$, 84520-95-6; C_2H_4, 74-85-1; CO, 630-08-0.

Hydrogen Bonding as a Probe of Electron Densities: Limiting Gas-Phase Nucleophilicities and Electrophilicities of B and HX

A. C. Legon*† and D. J. Millen*‡

Contribution from the Department of Chemistry, University of Exeter, Exeter EX4 4QD, England, and Christopher Ingold Laboratories, Department of Chemistry, University College London, London WC1H OAJ, England. *Received July 7, 1986*

Abstract: Hydrogen-bond stretching force constants (k_σ) determined from the rotational spectra of dimers B···HX have been used to establish the nucleophilicities (N) of B for B = N_2, CO, PH_3, H_2S, HCN, CH_3CN, H_2O, and NH_3 and the electrophilicities (E) of HX for X = F, Cl, CN, Br, C≡CH, and CF_3. Values of E and N have been used to predict k_σ for a number of dimers as yet unobserved.

I. Introduction

Chemists have long recognized the desirability of predicting the strength of binding in a hydrogen-bonded dimer B···HX (or other weakly bound species) from the properties of the component molecules B and HX. In this article, we show how to establish limiting, gas-phase nucleophilicities (N) and electrophilicities (E) of the components B and HX in a simple manner from a readily determined spectroscopic property, namely, the hydrogen-bond stretching force constant, (k_σ). The quantities N and E can then be used to predict the strength of binding (as measured by the force constant k_σ) for a large number of dimers. The theoretical foundation of this procedure is discussed in terms of recent electrostatic modeling of the hydrogen bond.

As a result of the investigation of a large number of hydrogen-bonded dimers by rotational spectroscopy,[1] it has become possible to enunciate some simple, essentially electrostatic rules for predicting the angular geometries of dimers.[2] In particular, at equilibrium the HX molecule lies along the axis of a nonbonding electron pair on B. In more general terms, we might speak of the most electrophilic site of HX (i.e., the H atom) seeking the most nucleophilic site of B, but of course the nucleophilic end of HX will avoid this site on B. (We are thus using the terms *nucleophilicity* and *electrophilicity* in the etymologically exact sense. The electrophilicity of the H atom in HX is therefore a measure of its capacity to seek out a particular (unperturbed) electron-rich region on a standard molecule B. We have deliberately used the qualification "limiting" in discussing E and N to draw attention to the fact that they are derived from measurements in weakly bound dimers and that this usage therefore differs from the more common but less literal view of the terms which is restricted to the extreme case of group transfers during chemical reaction.) The electrostatic approach to hydrogen bonding has received a quantitative interpretation by Buckingham and Fowler[3] who use a distributed multipole analysis to predict angular geometries. Rotational spectroscopy, as well as leading to geometries, has also provided hydrogen-bond stretching force constants (k_σ) for many dimers B···HX.[4] A comparison of k_σ values within a series gives a measure of the relative strength of the dimers which are, moreover, in isolation in the gas phase. It is timely to interpret the k_σ values in terms of the properties of the individual components B and HX in a way that employs an analogous approach to that used for angular geometries, i.e., the concepts of nucleophilicity and electrophilicity.

II. Limiting, Gas-Phase Nucleophilicities and Electrophilicities.

The success of the nonbonding electron-pair model in predicting angular geometries of B···HX and the weakness of the intermolecular interaction when considered together provide the basis for scales of limiting, gas-phase nucleophilicity and electrophilicity. For a dimer of a given geometry, the strength of the interaction will then depend on the magnitude of the nucleophilicity of the site on B and the electrophilicity of HX but nevertheless will usually be sufficiently small to be described by the electrostatic model involving essentially undistorted charge distributions in B and HX (see below).

One common measure of the strength of binding in dimers is the dissociation energy, but this is rarely available. Recently, it has been shown how realistic values of the quadratic force constant (k_σ) for stretching the weak bond in B···HX can be calculated from the centrifugal distortion constants D_J or Δ_J obtained experimentally.[5] Consequently, a large number of k_σ values are now in the literature.[4] We therefore collect in Table I this quantity[6-35] for the series B···HX where B = N_2, CO, PH_3, H_2S,

† University of Exeter.
‡ University College London.

(1) Legon, A. C.; Millen D. J. *Chem. Rev.* **1986**, *86*, 635.
(2) Legon, A. C.; Millen, D. J. *Faraday Discuss. Chem. Soc.* **1982**, *73*, 71.
(3) Buckingham, A. D; Fowler, P. W. *Can. J. Chem.* **1985**, *63*, 2018.
(4) Legon, A. C.; Millen, D. J. *Acc. Chem. Res.*, in press.
(5) Millen, D. J. *Can. J. Chem.* **1985**, *63*, 1477.

0002-7863/87/1509-0356$01.50/0